New fully functioning digital hologram recording system and its applications

Der-Kuan Kang
T-Security Incorporated
1179 Beekman Road
Hopewell Junction, New York 12533

Miguel Alcaraz Rivera
Javier Báez
María Luisa Cruz-Lopez
Instituto Nacional de Astrofísica
Óptica y Electrónica
Luis Enrique Erro # 1
Tonantzintla, Puebla, México 72840
E-mail: repepinoptero@gmail.com

Abstract. We propose a low-cost optical system that is able to simply generate computer-generated holograms and rainbow type and true-color Lippmann type holograms. In this system, a microimaging system is applied to reduce the digitized optical data/patterns to achieve about 0.45 μm of optical resolution for rainbow hologram recording and an about 60-deg viewing angle for the Lippmann hologram. The system is designed as a turn-key machine switching between different operating modes. Custom-generated software is applied to calculate and write digital fringe patterns at real-time speed. Applications for the digital rainbow hologram include computer-generated holograms, anticounterfeiting security labels, 3-D display, and 2-D/3-D truecolor holographic stereogram images for the Lippmann hologram. This single-process synthesizing system can be considered as a fully functioning hologram printer. [DOI: 10.1117/1.3497068]

Subject terms: holography; digital rainbow hologram; Lippmann holographic stereogram; computer-generated hologram, kinoform; fringe writer; hologram printer.

Paper 090779PRR received Oct. 9, 2009; revised manuscript received May 17, 2010; accepted for publication Aug. 25, 2010; published online Oct. 26, 2010.

1 Introduction

Holography has found a place among other security and display technologies, and new techniques to create holograms have been introduced since its invention.[1,2] This paper discusses a technology for making a master hologram for printing applications. Some of these technologies focus on the enhancement of the image quality and recording flexibility of holograms, and some computer-aided synthesizing methods have been reported.[3–5]

These methods include among others, dot matrix recording and *e*-beam writing. For the former, two laser beams are used to create small dots, of a particular size with a simple interference pattern, that work as hologram elements. Each hologram element has a grating with a specific period recorded, and this homogeneity inside leads to a limit on its image resolution. The *e*-beam writing system has been successfully applied to security label printing and has the capacity to create high-diffractive-efficiency images because of its ultrahigh optical resolution, which could achieve holograms with up to 2.5×10^4 dpi (dots per inch) resolution.[6] It is also used to create CGHs computer-generated holograms (CGHs), kinoforms, diffractive optical elements, etc.[7]

Both of these techniques provide a single-step procedure to record the relief gratings that shape the digital holograms. However, the image resolution and recording flexibility issues in the dot-matrix technique, and the high cost of equipment and slow writing speed issues in the *e*-beam method remain subjects for improvement.

Another approach to a single-step recording procedure was proposed for a true-color 3-D Lippmann hologram, where computerized data is used to record the hologram.[8] However, it still lacks the level of fine customization of the CGH or the digitalized relief type (rainbow type) hologram recording features, and remains a single-function-machine with a high cost issue.

To provide a complete solution for the issues just described, a new optical recording setup is proposed and practically built. This new recording system incorporates a digital 2-D/3-D (2-dimensional and 3-dimensional combination) rainbow hologram writing function with an *e*-beam-equivalent resolution and 2-D/3-D true-color Lippmann hologram printing. Both can be directly generated in one single step from a single imagery art design through a PC-controlled system.

2 Optical Setup

Two things are important to consider when designing a new optical setup capable of recording a digital rainbow hologram and a true-color Lippmann hologram. One is the difference in optical resolution and the other is the flexibility of operation between both recording modes. Figure 1 shows a diagram of the designed setup that contains an image pattern/phase display SLM (spatial light modulator) unit, a microimaging zoom lens setup, and an autofocusing unit.

In this optical setup, calculated optical data are displayed on the SLM and further reduced in size by approximately $50\times$ reduction, then imaged over the recording material. The holographic plate is transported using an *XY* stage with submicrometer control repeatability. The entire imaging lens setup is well designed to move up and down together with an SLM panel through a real-time-response autofocusing unit. This unit maintains the conjugation point of the input image plane over the photosensitive material plane with submicrometer-order accuracy.

A laser beam is collimated and propagated into a random phase generator that eliminates the coherent speckle noise produced by dust and imperfections in the optics. The random phase generator used is a phase-controlled modulator from Displaytech Inc. called SLM1 with a pixel pitch of 15 μm (Fig. 1). SLM1 is also used as a

0091-3286/2010/$25.00

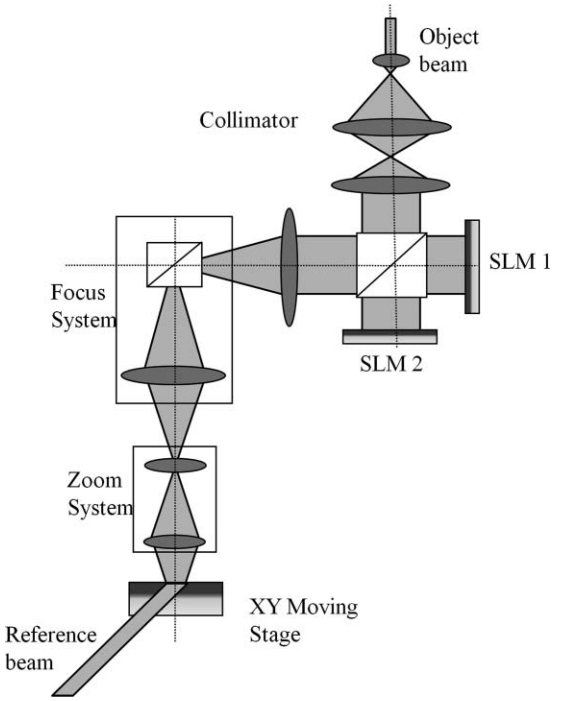

Fig. 1 Basic optical setup for both digital rainbow and true-color Lippmann hologram recording.

specified phase generator when it is necessary to digitally add phase information to the final optical output. The wavefront after SLM1 is further reflected into a second SLM; a time- and amplitude-controlled SLM from Texas Instruments with a pixel pitch of 13 μm (Fig. 1) where the calculated amplitude image is displayed and then projected onto the photosensitive material surface. The image displayed in SLM2 with a total of 1024×768 pixels, is reduced to a size of 200×150 μm and projected as an exposed element onto the material surface.

The optical recording resolution of the optical setup is based on the numerical aperture (NA), given by

$$\mathrm{NA} = \sin\theta = \frac{D}{2f}, \tag{1}$$

where θ is the angle, D is the diameter of the entrance pupil, and f is the focal length.

With a resulting NA of 0.45, we can achieve an approximately 0.4-μm meter resolution. For a plain grating recording, this means one line pair can be achieved in 0.8 μm and forms up to 1200 line pairs/mm.

As mentioned, each exposed cell has a size up to 200 μm containing 1024×768 pixels of digitized data. It is reasonable to divide it into a subcell matrix, using programming techniques to achieve higher image resolution until the smallest subcell reaches one line pair. In this case, the highest image resolution for a plane grating is about 2.5×10^4 dpi, and 1200 line pairs present a 40-deg off-axis hologram. For a color 3-D image using plain grating technique,[4,5] the image resolution is limited to about 1500 dpi since the area is divided to display the R, G, and B color components and perspective views. To preserve this high resolution, an autofocus system is also present as part of the general layout. This part of the system enables it to maintain every image in focus, avoiding the errors that could result from platform movements.

2.1 *Digital Rainbow Hologram Recording Mode*

Optical data and fringe patterns are calculated in advance in the recording mode of digital rainbow hologram or computer-generated rainbow hologram.[9] The output data are directly printed over a photoresist through the setup shown in Fig. 1, while the reference beam is blocked and not used in this method. The fringe patterns are produced by optimized etching depths over the photoresist layer. A dedicated processor makes the necessary calculation of the fringes based on a 2-D 8-bit gray-scale map. The 2-D gray-scale map works as a designed look-up map that indicates an optical feature to be present in the output hologram. An overview art map design gives the user an idea of the final result and works by indicating the software where each effect is located. Additionally, for each effect, a more detailed gray-scale map indicates with each of the 256 gray tones, a different special frequency that will build the fringe pattern in the hologram if the selected effect is a rainbow hologram. In a feature where a more complex pattern is to be recorded, as is the case for microtext or diffusers, the gray scale represents an actual variation of intensity for the beam to obtain the corresponding etching depth in the recording that will build the desired pattern.

Other feature choices include a 2-D plain grating image, a 3-D grating image, or a kinoform pattern. The simulated optical data representing these features is taken in small cells of pixels, and each cell can be further subdivided into smaller parts to reach the optical limitation, to achieve the mentioned resolution of 2.5×10^4 dpi. A diagram of this process is shown in Fig. 2. The cells are then displayed on SLM2 (Fig. 1) for further recording as a hologram over a thin photoresist layer.

The look-up map makes it easy to record various patterns in the same output work, which is not limited to fringe patterns but also can combine features such as microtext, logotypes, etc. and CGHs. Submicrometer precision is reached in the alignment of adjacent exposures with the XY stage movement to avoid gaps and defects between the blocks.

2.1.1 *Optimization of diffraction efficiency*

Maximizing the diffraction efficiency of a relief-type hologram is a critical part of the process. It is affected by the emulsion thickness among other parameters. Equation (2) presents the relationship between diffraction efficiency pa-

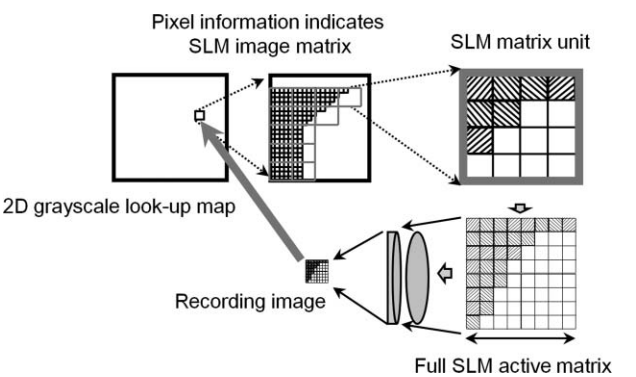

Fig. 2 Diagram of gray-scale map transformation to a recording image.

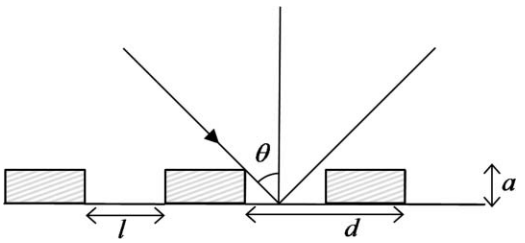

Fig. 3 Grating profile and diffraction efficiency.

rameters for a relief profile grating that is introduced from Fourier transform theory as

$$\eta = \left(\frac{2}{\pi}\right)^2 \sin^2\left(\frac{\pi n a}{\lambda \cos\theta}\right) \sin^2\left(\pi \frac{l}{d}\right), \tag{2}$$

where n is the refraction index of the material, θ is the reconstruction beam angle, λ is the wavelength used for the reconstruction, a is the depth of the grating, d is the period of the grating, and l is the length of the etched part, as shown in Fig. 3.

Equation (2) gives the conditions to achieve maximum diffraction efficiency, which can be expressed as

$$d = 2l \text{ and } a = \frac{\lambda \cos\theta}{2n}. \tag{3}$$

For a typical photoresist material with a refraction index around 1.64 in the visible wavelength, the optimized depth a is about 0.16 to 2.2 μm. Equation (3) provides the optimization fringe pattern design and material etching conditions for maximum efficiency in digital rainbow recording.

2.2 *True-Color Lippmann Hologram Recording Mode*

It is simple to switch the optical setup from relief hologram recording mode to reflection-type hologram recording mode using the setup shown in Fig. 1, making it possible to record 3-D stereographic volume holograms. In rainbow holograms, however, the high definition of the recorded images oblige the system to focus carefully on the recording substrate. In this mode, any focus plane will work, given that all the phase information is recorded, so the zoom lens unit can be automatically adjusted by computer control to shift the focal plane of the SLM image to a plane close to the plate with the intention of making the spot on the substrate the desired size. The focal plane shifting also gives a fine homogeneous energy distribution to the volume emulsion for a better dynamic range control to the material sensitivity. The propagation of the wavefront coming from the SLM and a reference beam incident from the opposite side form a volume fringe pattern as a holographic element.[8] The size of the element is limited by the energy distribution between the object and the reference beam. The maximum viewing angle of the reflective hologram is determined by the NA of the optical setup, 0.45 in this cases, and achieves an about 60 deg viewing angle.

A light source chamber containing three color lasers is introduced in the same optical path to obtain a full-color hologram. The lasers utilized were a helium-neon laser for the red color (633 nm) and diode-pumped solid state lasers for green (532 nm) and blue (457 nm). In this recording mode, instead of the random phase modulation introduced

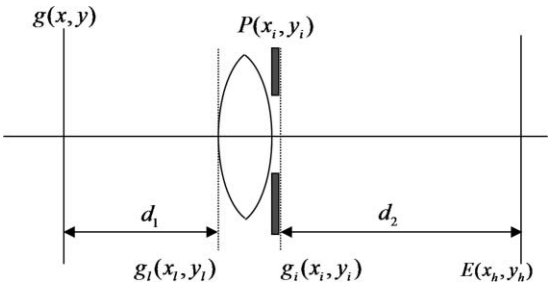

Fig. 4 Basic single-lens optical model of a rainbow CGH.

using SLM1 in digital rainbow recording mode (Fig. 1), it is feasible to use the same equipment to apply modulated phase information to enhance the image quality.[10] Only the size of the *XY* stage limits the theoretical size of the final hologram in this mode, because any number of views can be obtained from a 3-D model and recorded as holographic elements.

3 Experimental Results and Applications

3.1 *Multiaperture White Light True-Color 3D CGH*

One of the advantages of using the system is its capacity to generate a custom wavefront through a CGH. In our experiments, to simply test the created wavefront, we considered a mathematic model simulating a white light 3-D stereogram.[11]

As shown in Fig. 4, the function $g(x, y)$ represents the original image as an initial wavefront that is propagated a distance d_1, then goes through a lens with focal length f and an aperture $P(x_i, y_i)$, and then is propagated a distance d_2. The resulting wavefront is expressed by the function $E(x_h, y_h)$. The function $E(x_h, y_h)$ can then be added to a reference wave to obtain the final interference pattern using Lee's method for encoding the phase and amplitude data into a binary pattern.[12]

The equation of the model is

$$E(x_h, y_h, \lambda_m) = \frac{1}{j\lambda_m d_2} \exp\left[jk_m\left(d_2 + \frac{x_h^2 + y_h^2}{2d_2}\right)\right] \times F\left[g_1(x_i, y_i) \exp\left(jk_m \frac{x_i^2 + y_i^2}{2d_2}\right)\right]. \tag{4}$$

Equation (4) includes a λ_m parameter, where m can vary to create a full-color effect. The variable k_m is the wave number, which is $2\pi/\lambda_m$; $g_i(x_i, y_i)$ is the propagation function of $g(x, y)$ after it goes through the aperture $P(x_i, y_i)$ and is given by

$$g_i(x_i, y_i, \lambda_m) = \frac{1}{j\lambda_m d_1} \exp\left[jk_m\left(d_1 + \frac{x_i^2 + y_i^2}{2d_1}\right)\right] \times F\left[g(x, y) \exp\left(jk_m \frac{x^2 + y^2}{2d_1}\right)\right] \times \exp\left(-jk_m \frac{x_i^2 + y_i^2}{2f}\right) P(x_i, y_i), \tag{5}$$

Equation (5) includes the aperture function $P(x_i, y_i)$ limited in the y direction, a key component of rainbow holography, and its existence enables the hologram to be seen in a white light ambient illumination.[13] Also, the $P(x_i, y_i)$

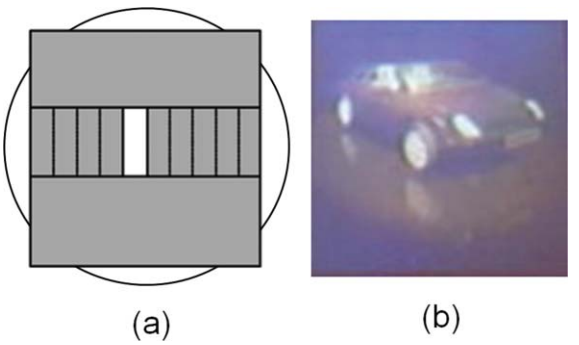

Fig. 5 (a) Aperture $P(x_i, y_i)$ provides perspectives views and a white light CGH in reconstruction and (b) 3-D color image in white light playback. (Color online only.)

function provides the ability to encode perspective views by shifting its position in the x direction [Fig. 5(a)]. Eight perspectives of 256×256 pixels were used in the experiment, and a 10-×10-mm color autostereoscopic 3-D hologram was obtained, as shown in Fig. 5(b).

3.2 *Anamorphic One-Step 3D True-Color CGH*

Another simulated optical setup to obtain a 3-D effect uses an anamorphic one-step holographic stereogram,[14,15] which consists of a lens setup with different focal length on the x axis (f_x) and the y axis (f_y), respectively. As shown in Fig. 6, the objective of this optical setup is to horizontally focus a 2-D image on the focal plane f_x, and vertically focus it on the focal plane f_y. In a real optical system, the perspective images are projected and focused to real images right behind the lens setup. In our digitized mathematic model, it is assumed that perspective images are propagated from the plane right after the virtual lens setup, as shown in Fig. 6. The wavefront is transformed in the x and y directions with f_x and f_y focal lengths, respectively. As a result, images are formed as a vertical line on the f_x focal plane and a horizontal line on the f_y focal plane, respectively.

The modeled setup can be expressed by

$$E(x_h, y_h) = \frac{1}{j\lambda f_x} \exp\left[jk\left(f_x \frac{x_h^2 + y_h^2}{2f_x}\right)\right] \times F\left\{G_l(x_i, y_i) \exp\left(-jk\frac{x_i^2}{2f_x}\right) \times \exp -jk\frac{y_i^2}{2f_y} \exp jk\frac{(x_i^2 + y_i^2)}{2f_x}\right\}, \quad (6)$$

where G_l is a bidimensional function containing one of the perspective views of the scene to encode, and λ is the wavelength of the source that will be used on reconstruction. The line formed in the f_x plane is then recorded on the hologram. Changing the design for a different view of the same object produces multiple slit views of the object, which can be recorded linedup one after another until a window of slits from the object is formed. These result in another case of an autostereoscopic 3-D hologram.

The preceding CGH data were calculated in such a way that the calculation and the printing can be completed at the same time, so it can be called a real-time calculation. This was achieved with a PC running Windows XP and a processor with a speed of 1.6 GHz. The complete writing process took 2 h to complete and make a 10-×10-mm sample with the resolution described in the optical setup. The 3-D stereoscopic effect was recognized in both of the preceding experiments.

3.3 *Display/Security Relief/Rainbow Hologram*

As already described, one of the important capabilities of the system is its application in security. Figure 7 presents a final design of various multiple digital data patterns that were calculated based on a single 2-D gray-scale look-up

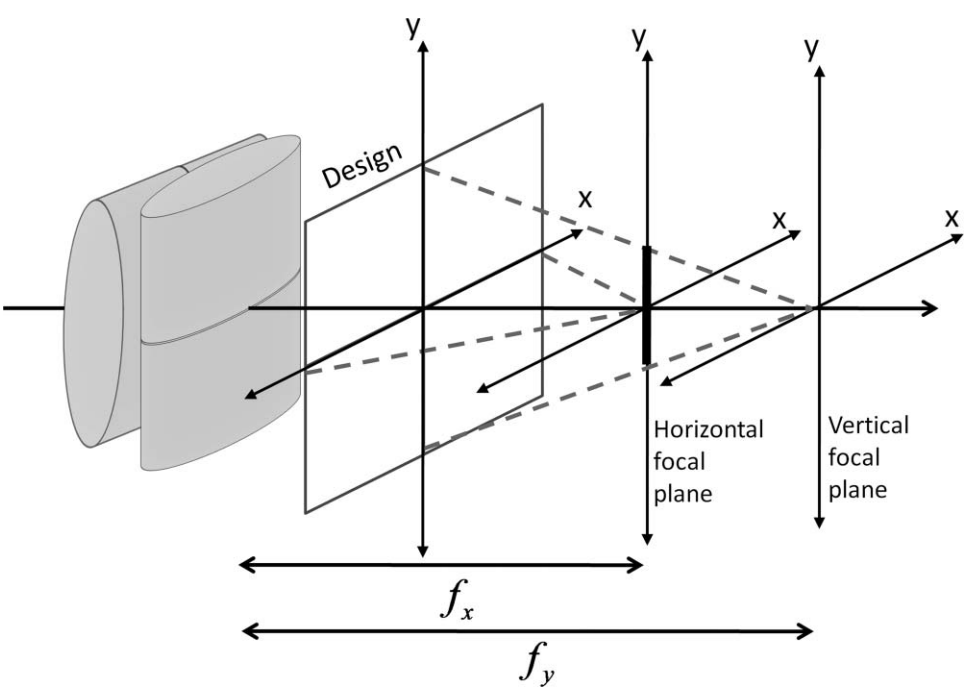

Fig. 6 Anamorphic lens model for recording a one-step stereoscopic CGH.

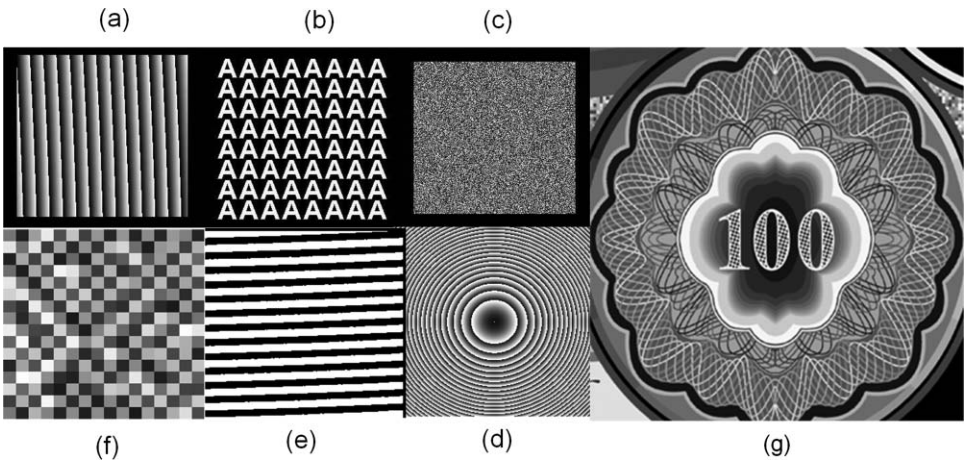

Fig. 7 Example patterns calculated and directly projected on to photoresist material based on single 2-D map: (a) blazed grating, (b) nondiffractive microtext, (c) directional diffuser, (d) microlens, (e) plain grating, (f) kinoform, and (g) example of 2-D gray-scale look-up map.

map. Figure 8 presents the final design, where the calculated data presented in Fig. 7 were used. The nondiffractive text/logo will measure 2 μm in height when printed, with 2.5×10^4 dpi image resolution. This will enable it to be detected only under a microscope with a magnification of 500×. The 1500 dpi full-color plain grating 32-view 3-D image with a speckle-free effect shows high quality and brightness.

3.4 *True-Color Full-Parallax Lippmann Holographic Stereogram Experiment*

Using the system volume hologram recording mode already described, a color portrait hologram and a CG hologram were successfully synthesized over a high-resolution thick polymer photoresist layer, as shown in Fig. 9. A series of 256×256 perspective images, each one containing 256×256 pixels, were further processed using an image-processing technique for full-parallax views that generalizes

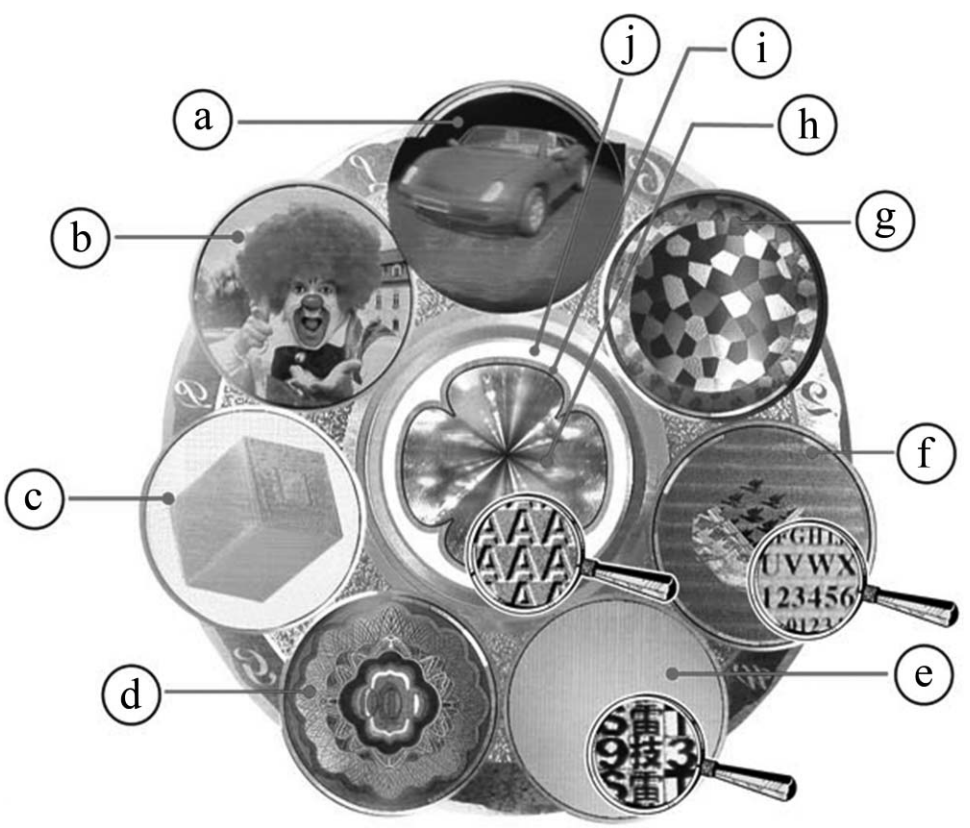

Fig. 8 Experimental sample that consists of various optical data: (a) 3-D autostereoscopic in color; (b), (c), and (g) rainbow hologram; (d) kinetic effect, (e), (f), and (i) microtext; (e) and (j) diffuser, and (h) lens effect.

Fig. 9 Reflective/Lippmann parallax true-color holographic stereogram with a real size of 16 cm^2: left, portrait; right, computer-generated bike.

from horizontal parallax-only processes.[14–16] The element hologram size reached was 100 μm in the samples; however, up to 50 μm could be experimentally achieved without seriously decreasing the diffraction efficiency.[8]

4 Conclusions

A low-cost automatic hologram synthesizing system was proposed and practically built as a prototype fully functioning printer for digital rainbow/relief type and Lippmann/reflective type holograms. In the former type, real-time fringe calculating software and a high-magnification microscopic system generated a variety of functions and security features in one hologram without a visible glitch or line gap. The system uses regular optical components in a special structured design; the entire system cost is much lower than an *e*-beam system and its operating procedure is more flexible.

Additionally, optical resolution adjustable from 0 to 1200 line pairs can be controlled by using software parameter inputs. A wide spectrum of applications, like 2-D and 3-D images, CGHs, kinoforms, microtext/logos, etc. were simply obtained based on a single look-up map design.

On the other hand, a tunable component was designed for switching between different operating modes: rainbow/relief hologram and true-color Lippmann/reflective hologram. Furthermore, a plug-in-type hybrid exposing-optical-head is doable to expand the system's specifications and applications. It is not necessary to readjust between different features once the system is properly adjusted and fixed. Therefore, it is possible to apply this system as a reliable fully functioning hologram printer for display or to develop optical device applications. Given the variety of hologram types the machine can produce and the ease of incorporating new original features via software or hardware adjustments, the machine can also be used to print security features that can adapt over time.

Acknowledgments

The authors would like to thank Mr. Hong Yang Su and the team members of T-Security, Inc., Taiwan. This research could not have been done without their support and encouragement.

References

1. L. Huff and R. L. Fusek, "Color holographic stereograms," *Opt. Eng.* **19**(5), 691–695 (1980).
2. G. Ackermann and J. Eichler, *Holography: A Practical Approach*, Wiley-VCH, Verlag GmbH & Co., Weinheim, Germany (2007).
3. C.-W. Tu, Y. A. Han, C.-K. Lee, J. W. Wu, A. S. T. Peng, E. H. Z. Liao, and J. T. Lee, "Expanding a color presentation range with true-color dot matrix holograms," *Proc. SPIE* **3637**, 130–140 (1999).
4. F. Iwata and K. Ohuma, "Grating images," in *Optical Security Systems, Proc. SPIE,* 12–14 (1988).
5. F. Iwata, "Grating image technology," *Proc. SPIE* **2577**, 66–70 (1995).
6. S. M. Arnold, "Electron beam fabrication of computer-generated holograms," *Opt. Eng.* **24**(5), 803–807 (1985).
7. L. B. Lesem, P. M. Hirsch, and J. A. Jordan, "The kinoform: a new wavefront reconstruction device," *IBM J. Res. Develop.* **13**, 150–155 (1969).
8. M. Yamaguchi, H. Endoh, T. Honda, and N. Ohyama, "High-quality recording of a full-parallax holographic stereogram with a digital diffuser," *Opt Lett.* **19**(2), 135–137 (1994).
9. H. Yoshikawa and H. Taniguchi, "Computer generated rainbow hologram," *Opt. Rev.* **6**(2) 118–123 (1999).
10. M. Yamaguchi, H. Hoshino, T. Honda, and N. Ohyama, "Phase-added stereogram: calculation of hologram using computer graphics technique," *Proc. SPIE* **1914**, 25–33 (1993).
11. M. Cruz-Lopez, M. Alcaraz, J. Baez-Rojas, and D.-K. Kang, "Holographic data calculating algorithm and new digital hologram recorder," *Proc. SPIE* **6488**, 648810 (2007).
12. W.-H. Lee, "Binary computer-generated holograms," *Appl. Opt.* **18**, 3661–3669 (1979).
13. H. Chen and F. T. S. Yu, "One-step rainbow hologram," *Opt. Lett.* (1978).
14. T. Honda, D.-K. Kang, K. Shimura, H. Enomoto, M. Yamaguchi, and N. Ohyama, "Large one-step holographic stereogram," *Proc. SPIE* **1461**, 156–166 (1991).
15. D.-K. Kang, T. Honda, M. Yamaguchi, and N. Ohyama, "One-step Lippmann holographic stereogram," *Proc. SPIE* **1667**, 127 (1992).
16. S. Maruyama, Y. Ono, and M. Yamaguchi, "High-density recording of full-color full-parallax holographic stereogram," *Proc. SPIE* **6912**, 69120N (2008).

Der-Kuan Kang received his MS and PhD degrees from Kyoto Institute of Technology and the Tokyo Institute of Technology in 1987 and 1991, respectively. He is currently working on research in security/display hologram applications with the R&D Department of T-Security, Inc., in New York. His research interests also include diffractive optical device and computer-generated holograms.

Miguel Alcaraz Rivera is working toward his PhD degree with the National Institute of Physics, Optics and Electronics (INAOE). He is currently working in the digital hologram field. His interests focus on computer processing and digital optics.

Jose Javier Baez Rojas received his MSc and PhD degrees from the Tokyo Institute of Technology, Japan, in 1991 and 1994, respectively. He is currently a researcher with the National Institute of Astrophysics Optics and Electronics in Mexico. His research interests include digital color, multispectral imagery, and digital image processing.

María Luisa Cruz López is currently finishing her Masters degree at the National Institute of Physics, Optics and Electronics (INAOE) in Puebla, Mexico, where she received her MS degree in optics in 2003. Her interests include holography, image processing, and computational simulations. She is a member of SPIE and the Optical Society of America.